Asymmetric Stable Deformations in Inflated Dielectric Elastomer Actuators

Lindsey Hines[1], Kirstin Petersen[2], and Metin Sitti[1]

Abstract— Robotic systems that are soft or incorporate soft actuators are well suited for operation in unstructured environments and for safe interactions with fragile objects. The majority, however, are tethered or burdened with bulky payloads of pumps and compressors. In a recent article we presented a sealed, inflated actuator composed of fluidically connected membrane dielectric elastomer actuators capable of large, repeatable, and stable deformations. Each membrane could switch between two identical volumes, and maintain its shape when an applied voltage was removed. Here we extend our previous work by simulating and demonstrating asymmetric stable deformations. In an experimental two-membrane setup, the membranes experience large and significantly different area strains of $>100\%$ and $>550\%$ when transitioning between stable states. With the addition of more membranes, this asymmetry can increase the number of discrete stable membrane sizes, allowing more complex control when later implemented in a mechanism.

I. INTRODUCTION

Soft actuators and systems comprise an exciting development in the field of robotics, coveted for their ability to operate in unpredictable cluttered environments, exhibit robustness to high impacts and chemicals, and facilitate compliant and safe interaction with fragile or living specimens while allowing inexpensive, simple manufacturing methods. Traditionally, most soft systems produce motion by shifting fluid around in flexible chambers using large compressors or pumps through tethers or bulky payloads. Naturally, these limitations have prompted research into methods for untethered operation. Examples of such recent work include the use of on-board air compressors [1], [2], micro-pumps [3], monopropellant liquid fuels [4], [5], or explosive fuels [6].

In a recent article, we demonstrated a different type of actuator capable of large, repeatable, and stable deformations of interconnected soft membranes in a single sealed pressurized chamber [7]. These deformations were achieved not by changing the amount of air in the system, but by utilizing a mechanical instability and modifying the elastic response of particular membranes using dielectric elastomer actuators (DEAs). A DEA is comprised of soft electrodes on either side of an elastomer membrane; when a high voltage potential is applied, the Coulomb force causes the electrodes to attract, effectively squeezing the material. DEAs require

high operating voltages, but low current and have low overall power consumption.

The idea of harnessing mechanical instabilities to create greater motion, force, or energy savings has prompted several recent successful robotic demonstrations [8], [9], [10]. Keplinger *et al.* was the first to utilize the snap-through instability of nonlinear hyperelastic materials in order to generate giant DEA strains [11], [12]. In the actuator methodology discussed here, we use this feature to create stable and repeatable shapes. These shapes remain even after power to the actuator is turned off. A well-known example of a nonlinear hyperelastic material can be seen in the common tubular latex balloon (Fig. 1(a)). When stretched these materials experience increasing stiffness, then softness, and finally increasing stiffness again. As such, at a certain range of internal pressures, two very different balloon inflation radii can coexist (Fig. 1(b)).

Our past work focused on the modeling and demonstration of symmetric deformations of an arbitrary number of fluidically connected identical DEA membranes [7]; here, we extend that work by simulating and demonstrating a two-membrane actuator capable of repeatable, asymmetric stable deformations by varying membrane thickness and area. One of the greatest inherent limitations of designing a system with discrete stable states is that the system is then limited to those configurations. With identical membranes each membrane will be either one of two sizes regardless of how many membranes are added to the system. Asymmetric stable states are more difficult to produce, but add the potential of many more sizes and varying configurations with the addition of more membranes. As indicated through several preliminary implementations shown in Section IV, Fig. 6,
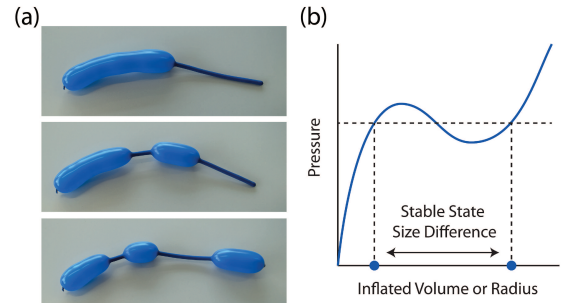

Fig. 1. Nonlinear hyperelastic materials, an example of which is the common latex tubular balloon (a). In (b) an illustration of an example balloon pressure-volume curve is shown. At a one pressure the balloon may locally be at one of two drastically different radii.

[1]Dr. L. Hines and Dr. M. Sitti are with the Max Planck Institute for Intelligent Systems, Heisenbergstrae 3, 70569 Stuttgart, Germany hines@is.mpg.de, sitti@is.mpg.de

[2]Dr. K. Petersen is with Cornell University, Ithaca, NY, 14853, USA kirstin@cornell.edu

pressurized dielectric actuators in general may be useful for a variety of robotic applications ranging from light weight, compact actuation of robot joints to, potentially, buoyancy control of underwater robots.

II. STABLE STATE DESIGN

There are several key components involved in the modeling and design of inflated dielectric actuators with multiple stable states. These include 1) membrane behavior upon inflation (i.e. the relation between inflated pressure and volume), 2) system equilibrium points and the number of stable states, and 3) whether state transitioning is possible. The details of the model are described in [7], and are briefly reiterated here. Our focus is on air-filled systems with fluidically connected, flat, circular membranes. The volume of each individual membrane is dependent upon the internal pressure and applied voltage; the fixed chamber connecting them has a constant volume.

A. Numerical Modeling

In clamped, inflated circular membranes, stress and strain vary from the membrane apex to its fixed edges. Therefore, to predict membrane shapes, a numerical approach is required. Here, functions relating pressure to volume, $p_i(V_i)$, for membrane i were found using the method described by Li *et al.* in [12]. Given material dependent hyperelastic model parameters and knowledge of the internal pressure, we can use the shooting method to predict membrane volume. This approach also considers the effect of the DEA applied voltage, which will influence the resultant pressure to volume function.

In a closed, inflated system it can be assumed that the number of filling molecules N remains constant. In addition, at equilibrium, the pressure throughout the system must be equal. These conditions allow us to write a set of equations that, when satisfied, are system equilibrium points:

$$N = \sum_{i=1}^{n} N_i + N_c, \qquad (1)$$

$$p_1(V_1) = p_2(V_2) = ... = p_i(V_i) = p_c(V_c), \qquad (2)$$

where n is the total number of membranes used, N_i denotes the number of molecules filling the volume enclosed by membrane i, and V_c is the constant internal volume of the connecting chamber. The values of $p_i(V_i)$ are given relative to atmospheric pressure. The terms N_c and $p_c(V_c)$ represent the number of molecules and the pressure in the fixed chamber connecting the membranes with a volume V_c. Assuming that the system is filled with air, and that the air acts as an ideal gas, these variables are related by

$$N_i = \frac{(p_i(V_i) + p_a)V_i}{kT}, \qquad (3)$$

where k is the Boltzmann constant equal to 1.38×10^{-23} J/K, T is the temperature taken to be 295 K, and p_a is the atmospheric pressure. The total number of molecules in the system, N, is assumed to be known and is based on the initial system pressurization.
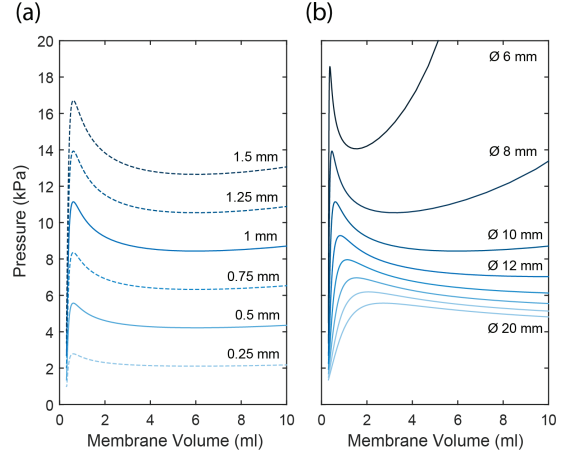

Fig. 2. Simulated acrylic elastomer membrane inflation, with internal pressure plotted with respect to membrane volume. a) A circular membrane with a diameter of 10 mm simulated with varying initial membrane thicknesses. Solid lines denote which thickness are commercially available through 3M. b) A 1 mm thick circular membrane simulated with varying diameters.

A numerical optimization routine can be used to solve eqns. (1)-(3), which must cover the search space carefully in order to find all solutions. Alternatively, in a two membrane actuator a graphical solution method can be used for a clear depiction of the system equilibrium points. Following [13] with some modifications, eqns. (1)-(3) can be formulated such that $p_1(V_1)$ and $p_2(V_2)$ are functions of a common variable, chosen to be N_1. For membrane volume ranges $V_1 = [0, V_{1max}]$ and $V_2 = [0, V_{2max}]$, the coordinates of the newly plotted curves (x_1, y_1) and (x_2, y_2) for membranes 1 and 2 can be written as

$$(x_1, y_1) = \left(\frac{(p_1(V_1) + p_a)V_1}{kT}, p_1(V_1) \right) \qquad (4)$$

$$(x_2, y_2) = \left(N - \frac{(p_2(V_2) + p_a)(V_2 + V_c)}{kT}, p_2(V_2) \right) \qquad (5)$$

where the pressure in fixed chamber is assumed to be equal to $p_2(V_2)$. The intersection of these two curves are equilibrium points of the system. Point stability can then be determined numerically by examining system perturbations within a small neighborhood.

Even if multiple stable equilibrium points exist, there is still no guarantee that the actuator will be able to transition between them. When a membrane is activated and a voltage is applied, the membranes must shift into new basins of attraction, the success of which is highly dependent upon the membrane material properties, size, total internal volume, and initial pressure. Comparison of the equilibrium points in both cases (where no voltage is applied, and where one or more membranes are activated) will predict whether this transition is possible.

B. Asymmetric Stables States

In an actuator with identical membranes, any existing stable equilibrium points will be symmetric barring any

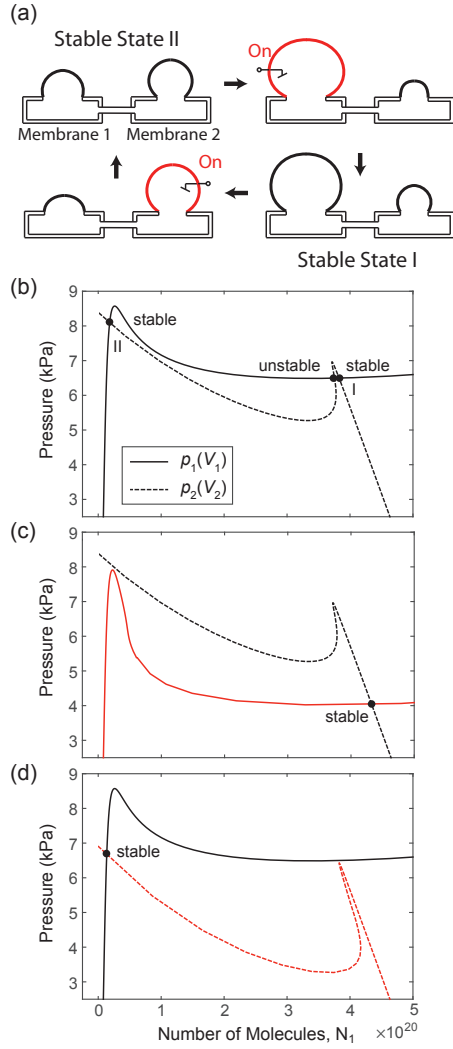Fig. 4. Experimental setup of the asymmetric, inflated, two membrane actuator

Fig. 3. Simulated two-membrane actuator with two asymmetric stable states. (a) Illustration of the process of switching between stable states. (b-d) Pressure to volume functions of two membranes plotted using eqns. (4) and (5). The function $p_1(V_1)$ corresponds to membrane 1 with a circular diameter of 13 mm and a thickness of 1 mm; $p_2(V_2)$ corresponds to membrane 2 with a circular diameter of 8 mm and a thickness of 0.5 mm. The solid line and dotted line represent membrane 1 and 2 respectively; the red color represents when voltage is applied to each membrane. In (b) no voltage is applied, and the system has a total of three equilibrium points and two stable states (I and II). In (c) 3.8 kV is applied to membrane 1 and in (d) 1.9 kV is applied to membrane 2.

viscoelastic effects. For example, in the inflated tubular latex balloon shown in Fig. 1, the radius can assume a large or small value, and varies only in specific location along the balloon length. If we can show that it is possible to transition from one stable configuration to another, we know that all other transitions are possible.

In the case of asymmetric coupled membranes this is not guaranteed; switching to a particular stable state may be irreversible. Despite these added design complications, using asymmetric membranes allows more complex motions and a broader range of robotic applications. Generally, asymmetric coupled membranes may achieve an increase in the num-
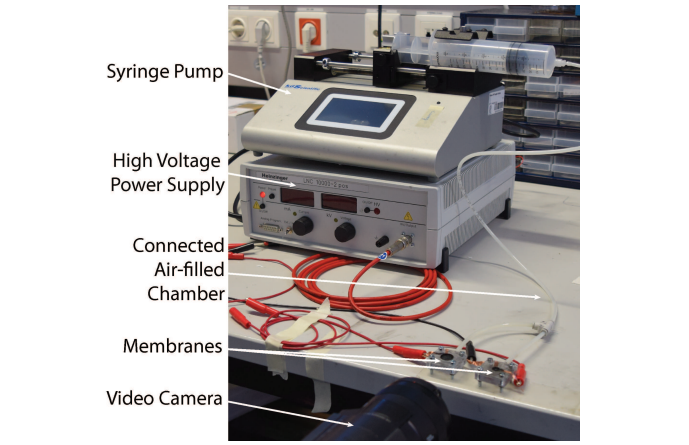
ber of discrete deformations, membrane linear displacement differences, and total system internal volume changes.

To enable asymmetric states, the inflation characteristics of the membranes must differ. Functions $p_i(V_i)$ will vary based on a number of parameters including membrane material, membrane thickness, size, and shape. Here we assume that the membranes remain flat, clamped circles and are composed of VHB acrylic elastomer tape from 3M. This material is widely used in dielectric actuators due to its high dielectric constant, high dielectric breakdown strength when strained, low elastic modulus, and highly nonlinear behavior when stretched [14], [15]. Even with this restricted design space, modifying only membrane circular radius and thickness is sufficient to generate significantly different inflation behavior. Figure 2 depicts a series of simulated functions $p_i(V_i)$ for a range of varying membrane parameters. Curves are generated through the approach described above, using the Gent hyperelastic material parameters of $\mu = 29.1$ kPa and $J_m = 228.4$ found through experimental fitting in [7].

C. Simulated Example

Here we examine the simplest two membrane case in simulation. Using the system model and pretabulated pressure to volume functions, sets of functional system parameters can be predicted. The pressure to volume functions were generated for circular membranes of diameters ranging from 5 to 15 mm in increments of 1 mm, with thicknesses of 0.5 and 1 mm. A grid search of membrane sizes was performed, with membrane pairs checked for multiple stable states where the fixed chamber size and initial pressurization was allowed to vary. No specific performance criteria was optimized; only system functionality was examined. Figure 3 depicts an example of a valid solution where a actuator with two asymmetric stable states is capable of switching between them upon an applied voltage.

The simulated system is composed of two different acrylic elastomer membranes with thickness of 1 mm and a diameter of 13 mm, and a thickness of 0.5 mm and diameter of 8 mm respectively. The fixed volume of the attached chamber, V_c,
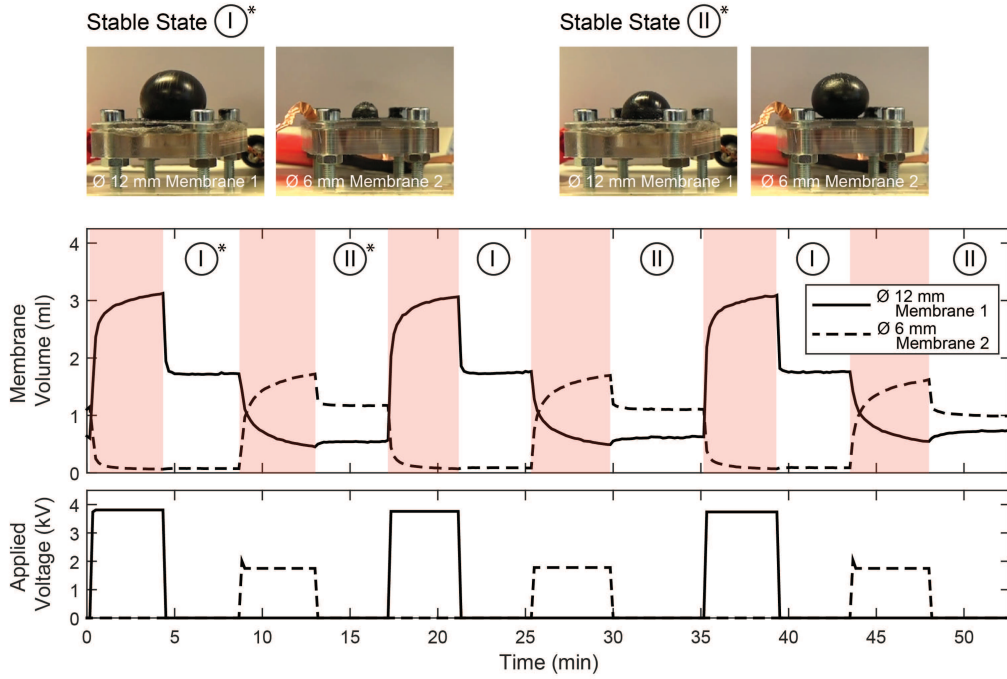
Fig. 5. Membrane volume and applied voltage over time in the inflated, two membrane actuator. Red bands indicate when the applied voltage is nonzero. Images of membranes are shown above in each of two stable states; alternating membrane activation allows the actuator to switch between them.

is 80 ml, and the total number of internal molecules, N, is $\sim 2.51 \times 10^{21}$. In Fig. 3(b-d) the pressure to volume functions of the two membranes are plotted using eqns. (4) and (5). As can be seen in Fig. 3(b), the system has three equilibrium points when no voltage is applied. Two of these points are stable, and the third unstable. Graphically, point stability can be more easily understood by examining the relative membrane pressures for a change in filling molecules N_1. For each equilibrium point, one can consider the case where the number of molecules in membrane 1 decreases or increases by δN_1. For example, if a decrease by δN_1 corresponds to a pressure in membrane 2 that is higher than membrane 1, this perturbation would be healed as the pressure stabilizes and molecules redistribute in the system, indicating that the point is stable. However, if the pressure in membrane 1 was greater than membrane 2, the perturbation would lead to a runaway process with N_1 continuing to decrease, indicating the point is unstable.

When a membrane is activated, the system's stability changes, leaving only one stable state. If initially at stable state II, activation of membrane 1 results in significant deformation as the system moves to its only stable configuration (Fig. 3(c)). The change is great enough such that the membranes are moved into a new basin of attraction and the system settles at state I when the voltage is removed. In this case the reverse is also true, as can be seen in Fig. 3(d), making the transition reversible and repeatable.

III. EXPERIMENTAL DEMONSTRATION

In order to show that asymmetric stable states and the ability to transition between them is reproducible outside

of simulation, a two membranes actuator is constructed and tested. Due to the viscoelastic nature of the acrylic elastomer and its effective softening upon recent and repeated stretches, the demonstrated actuator parameters differ slightly from those simulated, using 12 mm and 6 mm diameter membranes rather than 13 mm and 8 mm, details of which are described below. As such, a direct comparison between the simulated and experimental system performance is not made.

A. Experimental Setup

A labeled image of the experimental setup can be seen in Fig. 4. Two membranes are clamped within individual 3D printed holders, which are connected with tubing to make a single air-filled chamber. The total fixed internal chamber size is 47 ml. The number of internal molecules is $\sim 1.24 \times 10^{21}$, corresponding to an initial pressurization of ~ 6.5 kPa in 47 ml. Membranes 1 and 2 are acrylic elastomers with initial thicknesses of 1 mm and 0.5 mm (3M VHB 4910, 4905) respectively. Membrane 1 is clamped such that a circular portion of 12 mm in diameter is free to move and expand; similarly, the membrane 2 is clamped to a 6 mm diameter circle. A conductive grease (Nye Nyogel 756G) is used to create a flexible, conductive electrode on both sides of each membrane.

A syringe pump (KD Scientific) is attached to the system for initial pressurization. After the system is pressurized, the syringe pump is fixed and does not move. Voltage is applied across each membrane using a high voltage power supply (Heinzinger LC 10000-2pos), whose maximum is dependent upon the membrane thickness to prevent dielectric

breakdown, which was determined experimentally. A single membrane is activated at a time, after which all voltage is removed and the system is allowed to settle. Each step is held for at least 4 minutes.

Membrane size is recorded with a video camera (Sony HDR-CX900). Membrane inflated volume is calculated in later post processing using the projected membrane shape with the assumption that it is radially symmetric.

B. Results

As can be seen in Fig. 5, the two membrane actuator stabilizes at two distinct stable configurations with membranes of different sizes. The volumes of membrane 1 and membrane 2 are plotted over time; voltage is applied to alternating membranes at times marked with red bands. In stable state I, membranes 1 and 2 have volumes with average 1.7 and 0.1 ml respectively, with a standard deviation of $\pm < 0.05$ ml between cycles. In stable state II average volumes are 0.6 and 1.1 ml respectively, with a standard deviation of ± 0.1 ml between cycles. As a result, between the stable configurations, membrane 1 experiences an area strain of $>100\%$ and membrane 2 an area strain of $>550\%$. When activated they stretch even further, to $>150\%$ and $>750\%$ respectively.

IV. DISCUSSION

The motion demonstrated by the membranes is both significant as well as significantly different. While at its maximum, the achieved area strain does not match the highest values shown to date (1165% [16], 1692% [11], [12]), it is comparable, with the added advantage of being both repeatable and stable. Membranes differed in volume by 1.6 ml and 0.5 ml in each stable state and experienced a difference in area strain of $\sim 400\%$. Change in total system volume was small, however, with a marginal 0.1 ml measured.

While 3M's VHB is well suited for dielectric actuators otherwise, its viscoelasticity is a significant limitation in the practical implementation of system in its current form. It not only leads to history dependent softening, but also to long transition times between stable states. During each transition, the unactivated membrane must be given enough time to settle; if either has not moved into their new attractive region, the system will rebound into its previous configuration once voltage is removed. This limits the actuator to operation on the time scale of minutes, which is orders of magnitude longer than demonstrated with flat prestained membrane DEAs [15].

VHB's sensitivity to strain history also serves to influence the repeatability of stable states and complicates accurate system modeling. The cyclic operation shown here is close to ideal, with both membranes recently strained though not to the same extent. Correspondingly, the resulting stable states are quite consistent. Excessive resting time in either state will overly change the materials elastic response and affect the system's stable configurations and ability to transition. With these potentially changing pressure to volume functions, accurate system simulations are difficult. In this case this
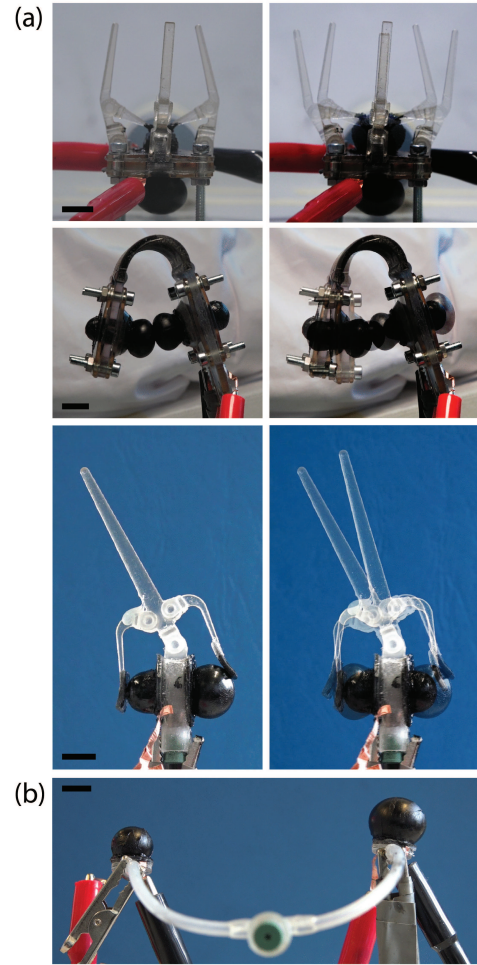

Fig. 6. Preliminary mechanism implementations using the inflated dielectric actuators in sealed chambers. Each scale bar represents 1 cm. (a) Mechanisms are pictured along side overlays illustrating maximum motion when when voltage is applied. (b) Deformation of low profile two membrane actuator connected with flexible tubing.

led to only an approximate prediction of which system parameters would succeed, where experimental membrane size was decreased to compensate for softening.

More accurate pressure to volume functions, with experimental pressure to volume curves or newly fitted hyperelastic model parameters for series of decreasing membrane sizes and stretching conditions, could help address some of these issues and allow more precise actuator design and further improvements. The development of new materials or new composite membranes without such viscoelasticity is another more difficult but more attractive option; while research on dielectric actuators has focused both on improving material dielectric constants and response times [15], [17], [18], [19], improving them in conjunction with material nonlinearity has not yet been a concern.

Even with these current limitations, the actuator can be incorporated into and used to drive various mechanisms. Figure 6 depicts a number of preliminary mechanisms where the membranes are used to produce motion. As long as they remain fluidically connected, membrane placement does not

matter, allowing a variety of configurations. Though current design constrains the system to flat circular membranes, which eases both modeling and implementation, generally speaking the described approach can be applied to membranes of other shapes and structure including continuous inflated tubes.

V. CONCLUSIONS

In this work we simulate and demonstrate an inflated actuator composed of two membrane dielectric actuators capable of repeatable, asymmetric stable deformations. In our experiment the membranes experienced significantly different area strains of $>100\%$ and $>550\%$ when transitioning between stable states. Future work includes implementation of a larger number of membranes, allowing an increase of the number of asymmetric stables states and discrete stable membrane sizes. In addition, characterizing actuator producible force and displacement when both active and stable is important, with the specific membrane loading point likely playing an important role in performance.

REFERENCES

[1] M. T. Tolley, R. F. Shepherd, B. Mosadegh, K. C. Galloway, M. Wehner, M. Karpelson, R. J. Wood, and G. M. Whitesides, "A resilient, untethered soft robot," *Soft Robotics*, vol. 1, no. 3, pp. 213–223, 2014.

[2] D. Yang, B. Mosadegh, A. Ainla, B. Lee, F. Khashai, Z. Suo, K. Bertoldi, and G. M. Whitesides, "Buckling of elastomeric beams enables actuation of soft machines," *Advanced Materials*, vol. 27, no. 41, pp. 6323–6327, 2015.

[3] S. Ueno, K. Takemura, S. Yokota, and K. Edamura, "Micro inchworm robot using electro-conjugate fluid," *Sensors and Actuators A: Physical*, vol. 216, pp. 36–42, 2014.

[4] C. D. Onal, X. Chen, G. M. Whitesides, and D. Rus, "Soft mobile robots with on-board chemical pressure generation," in *International Symposium on Robotics Research*, Flagstaff, USA, August 2011.

[5] M. Wehner, R. L. Truby, D. J. Fitzgerald, B. Mosadegh, G. M. Whitesides, J. A. Lewis, and R. J. Wood, "An integrated design and fabrication strategy for entirely soft, autonomous robots," *Nature*, vol. 536, no. 7617, pp. 451–455, 2016.

[6] R. F. Shepherd, A. A. Stokes, J. Freake, J. Barber, P. W. Snyder, A. D. Mazzeo, L. Cademartiri, S. A. Morin, and G. M. Whitesides, "Using explosions to power a soft robot," *Angewandte Chemie International Edition*, vol. 52, no. 10, pp. 2892–2896, 2013.

[7] L. Hines, K. Petersen, and M. Sitti, "Inflated soft actuators with reversible stable deformations," *Advanced Materials*, vol. 28, no. 19, pp. 3690–3696, 2016.

[8] J. T. Overvelde, T. Kloek, J. J. Dhaen, and K. Bertoldi, "Amplifying the response of soft actuators by harnessing snap-through instabilities," *Proceedings of the National Academy of Sciences*, vol. 112, no. 35, pp. 10 863–10 868, 2015.

[9] S.-W. Kim, J.-S. Koh, J.-G. Lee, J. Ryu, M. Cho, and K.-J. Cho, "Flytrap-inspired robot using structurally integrated actuation based on bistability and a developable surface," *Bioinspiration & biomimetics*, vol. 9, no. 3, p. 036004, 2014.

[10] M. Follador, A. Conn, and J. Rossiter, "Bistable minimum energy structures (bimes) for binary robotics," *Smart Materials and Structures*, vol. 24, no. 6, p. 065037, 2015.

[11] C. Keplinger, T. Li, R. Baumgartner, Z. Suo, and S. Bauer, "Harnessing snap-through instability in soft dielectrics to achieve giant voltage-triggered deformation," *Soft Matter*, vol. 8, no. 2, pp. 285–288, 2012.

[12] T. Li, C. Keplinger, R. Baumgartner, S. Bauer, W. Yang, and Z. Suo, "Giant voltage-induced deformation in dielectric elastomers near the verge of snap-through instability," *Journal of the Mechanics and Physics of Solids*, vol. 61, no. 2, pp. 611–628, 2013.

[13] I. Müller and P. Strehlow, *Rubber and rubber balloons: Paradigms of thermodynamics*. Springer, 2004, vol. 637.

[14] R. Pelrine, R. Kornbluh, Q. Pei, and J. Joseph, "High-speed electrically actuated elastomers with strain greater than 100%," *Science*, vol. 287, no. 5454, pp. 836–839, 2000.

[15] P. Brochu and Q. Pei, "Advances in dielectric elastomers for actuators and artificial muscles," *Macromolecular Rapid Communications*, vol. 31, no. 1, pp. 10–36, 2010.

[16] H. Godaba, C. C. Foo, Z. Q. Zhang, B. C. Khoo, and J. Zhu, "Giant voltage-induced deformation of a dielectric elastomer under a constant pressure," *Applied Physics Letters*, vol. 105, no. 11, p. 112901, 2014.

[17] G. Gallone, F. Galantini, and F. Carpi, "Perspectives for new dielectric elastomers with improved electromechanical actuation performance: composites versus blends," *Polymer International*, vol. 59, no. 3, pp. 400–406, 2010.

[18] D. M. Opris, M. Molberg, C. Walder, Y. S. Ko, B. Fischer, and F. A. Nesch, "New silicone composites for dielectric elastomer actuator applications in competition with acrylic foil," *Advanced Functional Materials*, vol. 21, no. 18, pp. 3531–3539, 2011.

[19] L. J. Romasanta, M. A. Lopez-Manchado, and R. Verdejo, "Increasing the performance of dielectric elastomer actuators: A review from the materials perspective," *Progress in Polymer Science*, vol. 51, pp. 188–211, 2015.